

Dielectric and Morphological Investigations of Phase Separation and Cure in Rubber-Modified Epoxy Resins: Comparison Between Teta- and DDM-Based Systems

COSTAS G. DELIDES,¹ DAVID HAYWARD,² RICHARD A. PETHRICK,^{2,*} and ARGYRIS S. VATALIS¹

¹Technological Education Institute (TEI) of Kozani, Laboratories of Physics and Material Technology, 50 100 Kila, Kozani, Greece; ²Department of Pure and Applied Chemistry, University of Strathclyde, Thomas Graham Building, 295 Cathedral Street, Glasgow G1 1XL, United Kingdom

SYNOPSIS

Real-time and equilibrium dielectric measurements, covering the frequency range 10^{-1} – 10^5 Hz, are reported on a series of rubber-modified epoxy resins, based on reaction of the diglycidyl ether of bisphenol A (DGEBA) with either triethylenetetramine (TETA) or diaminodiphenylmethane (DDM). The rubber modifier used was a carboxyl-terminated butadiene acrylonitrile (CTBN) reactive oligomer and the phase-separated structure, the results of which was examined using both dielectric and electron microscopic techniques. The mixture was initially homogeneous, but after a short period of time, it underwent phase separation and this process was marked by the appearance of a dielectric peak associated with ion-charge migration within the occluded rubbery phase. Analysis of the peak provided information on the morphology of the system and these data were compared with information obtained from scanning electron microscopy. A phase-separated morphology was observed consisting of spherical rubber particles dispersed in an epoxy matrix. For high concentrations of rubber ≥ 10 wt %, precipitation of epoxy domains within the rubbery phase was observed. Detailed dielectric studies of the peak associated with phase separation revealed that in the case of the TETA system the peak continued to shift after vitrification, whereas in the case of DDM, it was invariant with time. The point at which the peak appears was used to determine the time at which phase separation occurred. Differences observed in the lower temperature dielectric spectra were associated with variations in the form of the phase structure and possibly reflect different degrees of densification of the matrix. Good agreement was observed between the predictions of the Maxwell–Wagner–Sillers (MWS) theory and experimental observation for these systems. © 1993 John Wiley & Sons, Inc.

INTRODUCTION

The effectiveness of a thermoplastics as toughening agents in both thermoplastic and thermoset applications depends upon a number of factors, particle size being particularly important in controlling the brittle-tough transition (BT) temperature.^{1–6} Toughening is, in general, explained through crazing or shear yielding mechanisms, but cavitation in or around the impact modifier particle can also make

an important contribution to the overall process. The distribution in particle sizes within the cured matrix is therefore of importance in understanding the toughening mechanisms in these materials and the mean particle size has been shown to significantly influence the BT temperature.^{1,6} A wide range of thermoplastics and rubber particles has been studied as impact-toughening modifiers for thermosets.^{7–13} Carboxyl-terminated butadiene acrylonitrile (CTBN) has been used as a modifier for amine-cured epoxy resins and exhibits significant improvements in the toughening of such thermosets.^{14–18} Scanning electron microscopy (SEM) data indicate that phase separation between the CTBN

* To whom correspondence should be addressed.

and epoxy components occurs in the finally cured material, the rubber occurring as small occluded spheres randomly dispersed in the epoxy resin matrix.¹⁹⁻²¹

A recent study of the dielectric properties of a model system,²² consisting of ionically doped poly(ethylene oxide) domains dispersed in a polycarbonate matrix, demonstrated that the size and conductivity distribution of the *occluded* phases can be accurately described by the Maxwell-Wagner-Sillers (MWS) model.²³⁻²⁵ This study indicates that the dielectric technique has the potential of being applied to the *morphological* characterization of phase-separated polymer systems. Dielectric measurements have in recent years come to a new preeminence with their application to *in situ* monitoring of cure in polar thermosetting resins.²⁶⁻³¹ Observations of changes with time in the dielectric constant and loss have been correlated with variations in the microrheology and allow optimization of the cure in composite structures.^{28,30}

In this paper, application of the dielectric method for the characterization of the processes occurring during cure and description of the morphology using the MWS model will be considered.

EXPERIMENTAL

Materials

The epoxy resin used in this study was the diglycidyl ether of bisphenol A (DGEBA), supplied by Shell Co. {Epon 828}, $M_n \approx 380$ g/mol. The epoxy resin was cured with either 4,4'-diaminodiphenylmethane (DDM) obtained from Ciba Geigy, UK, or triethylenetetramine (TETA) obtained from British Drug Houses, Poole, Dorset. The rubber modifier, carboxyl-terminated butadiene acrylonitrile copolymer (10% AN) (Hycar CTBN 1300 × 15) was obtained from B. F. Goodrich Co., U.S.A.

Sample Preparation

The DGEBA was mixed with the CTBN in a glass vessel to give the required formulation, and to this was added the curing agent, either DDM or TETA,

Table I Conditions Used in Mixing the Resins

| Curing Agent (phr) | Temperature | Mixing Time |
|--------------------|-------------|-------------|
| TETA | Ambient | 3 min |
| DDM | 80°C | 10 min |

Table II Curing Conditions for Resins Systems

| Resin | Curing Agent (phr) | Cure Schedule |
|------------------|--------------------|----------------------------------|
| DGEBA (Epon 828) | TETA (20) | 2 h at 60°C |
| DGEBA (Epon 828) | DDM (HT972) (29.1) | 30 min at 100°C and 3 h at 180°C |

in stoichiometric amounts. The mixture was placed in a preheated oil bath to lower the viscosity and aid mixing, which was achieved by stirring until a clear fluid was obtained. The conditions used for mixing are presented in Table I. The mixture was degassed in a vacuum oven to remove trapped air. Curing of the mixtures were either performed in specially designed cells for the dielectric and rheological measurements or molded in glass containers. The latter molds consisted of glass plates of dimensions 6 × 6 cm separated by resin-coated glass laminate of the required thickness. The glass was cleaned with acetone and water and then dried. The surface was then treated with a release agent (Rocal MRS Advanced Non-Silicone Dry Film Spray). The plates were held together by toolmakers' parallel clamps and preheated to the required curing temperature and filled with resin by capillary action. Curing was carried out in an oven for the required amount of time (Table II). A number of samples were machined from these cured plaques.

Dielectric Measurements

Real-time Measurements

Dielectric measurements were performed using a Solatron 1250 Frequency Response Analyser (FRA); the method used for interfacing the instrument to the sample and the procedures used for data analysis have been described previously.³² Data were collected between 10^{-1} and 6.3×10^4 Hz in a period of less than 3 min. The system was programmed to store successive sets of data and allowed real-time examination of the cure process for all the mixtures. A cell was designed that consisted of two pre-etched copper electrodes mounted on an epoxy glass fiber base. This design generates a three-electrode system with an active electrode area of 1 cm² and was placed in an Oxford Instruments cryostat (DN1704). The space between the electrodes was maintained constant with a copper spacer, and the electrodes and spacer were soldered together to form a seal around

three edges. The resin to be studied was injected as a liquid into the cell, capillary action ensuring the cell was completely filled. The electrodes were in good thermal contact with a copper block that was used to maintain the temperature of the sample at that required for the isothermal cure studies.

Temperature-Dependent Measurements

Thin films of the rubber-modified thermoset, prepared according to the procedure outlined in Table II, were investigated over the temperature range -70 to 170°C using both the measuring system described above and an ANDO Electric TRS-10T Dielectric Loss Measuring Set composed of a TR-10C Dielectric Bridge, a WBG-9 Oscillator, a BDA-9 Null Detector, a TO-19 Thermostatic Oven, and a SE-70 Electrode Set.³³ The temperature was controlled with a precision of ± 1 K in both systems.

Scanning Electron Microscopy (SEM)

Scanning electron microscopy was performed using a SEM (JSM-840A) microscope. Fracture surfaces were obtained by bending the samples through 90° at room temperature and the surfaces generated sputtered with gold to reduce charging effects during examination.

Differential Scanning Calorimetry (DSC)

Small samples of the films obtained using the curing cycle (Table II) were placed in aluminum pans and thermal data obtained using a DuPont 910, differential scanning calorimeter (DSC) over a temperature range of -150 to 200°C at a heating rate of $10^{\circ}\text{C}/\text{min}$. Computer software provided with the instrument was used to determine the glass transition temperature, T_g . Traces were obtained both on heating and cooling and also after thermal annealing at a temperature above the T_g .

RESULTS AND DISCUSSION

The TETA/DGEBA and DDM/DGEBA systems mixed with CTBN have been investigated previously using the Strathclyde Curometer,³⁴ and suitable conditions for the investigation of the cure process in these systems identified. For TETA/DGEBA, the highly exothermic nature of the reaction indicates that 30°C is appropriate, whereas 80°C is more suitable for DDM/DGEBA. All the data presented here were obtained using these schedules.

Electron Microscopy

SEM micrographs of fracture surfaces for both DGEBA/TETA/CTBN and DGEBA/DDM/CTBN are shown in Figures 1 and 2. The smooth, glassy fracture surface for the unmodified epoxy [Figs. 1(a) and 2(a)] with cracks in different planes shows brittle fracture with parallel ripples. The ripples are fewer in the DGEBA/TETA than in the DGEBA/DDM system, consistent with a different fracture mechanism operating in the lower T_g TETA system.

The fracture surface of the rubber-modified epoxy systems has a rigid continuous phase with a dispersed rubbery phase of isolated spherical particles. The diameter of the particles is increased with CTBN concentration and it varies between 1.5 and $5.4\ \mu\text{m}$ for the DGEBA/DDM/CTBN and between 0.7 and $2.9\ \mu\text{m}$ for the DGEBA/TETA/CTBN. The average diameter of the rubber occlusions increases with cure temperature and amount of CTBN and the final morphology appears to be attained well before gelation or vitrification.³⁵⁻³⁷

For rubber concentrations higher than 10 wt %, small spherical epoxy domains are observed within the CTBN occlusions [Figs. 9(d)-(f) and 2(d)-(f)]. The extent to which these inclusions are observed increases with the CTBN concentration. Although previous studies^{19-21,35-37} reported similar conclusions with regards the size of the rubbery domains, they have not, with the exception of Pearson and Yu, highlighted the inclusion of the epoxy phase within the rubbery-phase structure. The occurrence of these inclusions does not appear to have been considered theoretically or in the interpretation of X-ray scattering studies of the phase-separation process.^{36,38}

Differential Scanning Calorimetry (DSC)

DSC measurements on the fully cured resins provided information on the variation of the T_g with composition of the rubber. It is known that the CTBN is thermodynamically compatible with the epoxy resin,^{8,14,38} and, hence, a depression of the T_g with addition of rubber would be expected. The data indicate a small decrease on the initial addition of CTBN, but the subsequent changes are more indicative of the materials existing as two separate phases (Table III). The system initially starts as a homogeneous mixture, and as cure proceeds, increases in the molecular weight of the resin lead to phase separation. How this process is achieved will obviously influence the resultant morphology and, in turn, can change the ultimate mechanical properties. In sys-

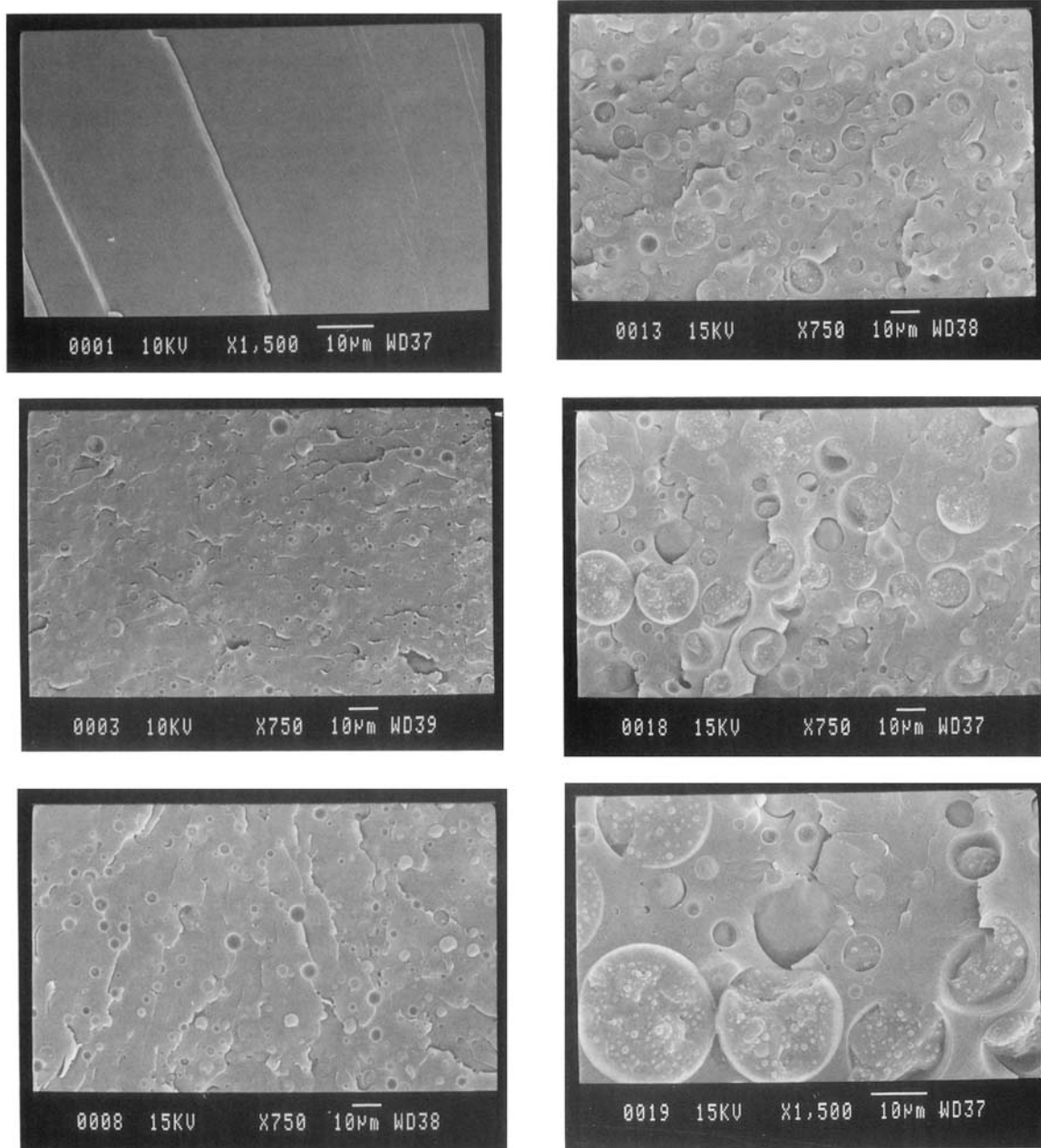


Figure 1 Scanning electron micrographs (SEMs) of fracture surfaces for the DGEBA/DDM/CTBN system. Amount of CTBN (wt %): (a) 0; (b) 5.2; (c) 10.6; (d) 16.2; (e) 16.2; (f) 22.6.

tems with a high rubber content (> 10 wt %), spinodal decomposition of the unreactive DGEBA/CTBN mixture will occur at temperatures below 50°C and at room temperature for compositions above 30 wt %.³⁸ Addition of the amine curing agent will significantly modify the phase diagram and initially raises the spinodal decomposition temperature. Subsequent changes in the molecular structure dur-

ing the cure reaction led to spinodal decomposition and generation of the observed phase structure (Figs. 1 and 2). The microscopic viscosity at the point of phase separation is sufficiently large to inhibit diffusion of the epoxy through the rubber and results in the generation of the occluded phases. These occluded phases have only a very minor effect on the value of the T_g ; however, they do influence the com-

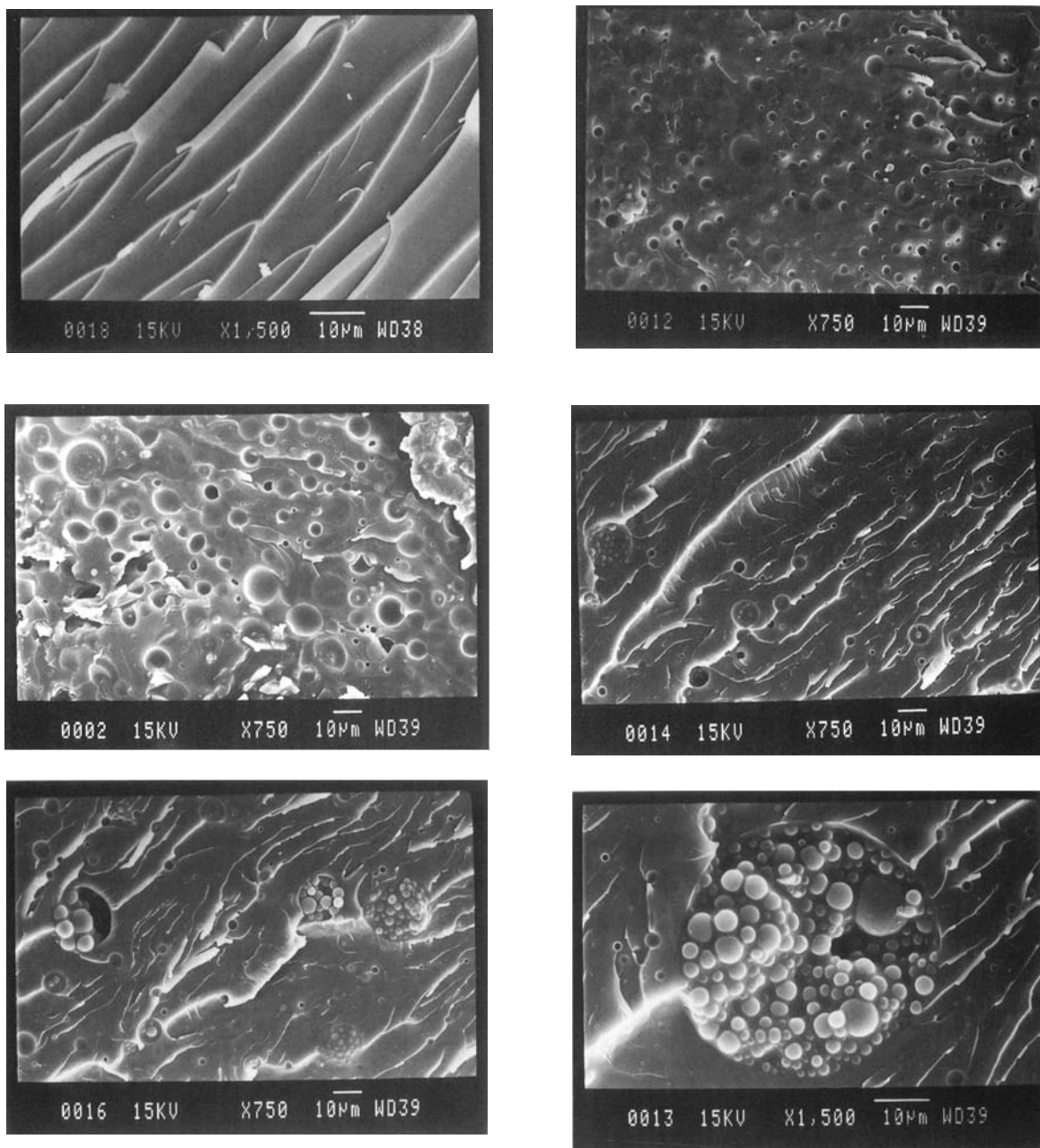


Figure 2 SEMs of fracture surfaces for the DGEBA/TETA/CTBN system. Amount of CTBN (wt %): (a) 0; (b) 5.2; (c) 10.6; (d) 16.2; (e) 16.2; (f) 22.6.

compressibility, as determined by ultrasonic measurement and the modulus of the final material.¹⁴⁻¹⁶ Below 10 wt %, a simple additivity law is obeyed for the compressibility, whereas above this concentration, there is a progressive deviation from ideal mixing and this continues up to the point at which phase inversion occurs.¹⁵ Inclusion of epoxy domains within the rubbery phase would lead to a reduction in the compressibility similar to that observed. The epoxy inclusions influence bulk properties, such as

the fracture energy, toughness, and compressibility, but have an insignificant effect on the microdynamics as reflected in the T_g . It is therefore of considerable interest to know at what point during cure this phase separation occurs.

Real-time Dielectric Measurements of Cure

Application of dielectric measurements to the characterization of cure have been reported previously

Table III Gelation and Phase-separation Times for DGEBA/TETA/CTBN and DGEBA/DDM/CTBN

| Resin DGEBA/ | CTBN (wt %) | Gelation Time (t_{gel}) (s) | |
|-------------------|----------------|---------------------------------|------------|
| | | Rheological | Dielectric |
| TETA ^a | 0 | | 15,600 |
| | 5.2 | | 10,820 |
| | 10.6 | | 10,200 |
| | 16.2 | | 9,800 |
| | 22.6 | | 10,200 |
| DDM ^a | 0 | 5,900 | 6,000 |
| | 5.2 | 4,520 | 4,320 |
| | 10.6 | 3,900 | 3,660 |
| | 16.2 | 2,940 | 2,880 |
| | 22.6 | 2,400 | 2,460 |

| Resin | CTBN (wt %) | Phase-separation Time (s) | |
|-------------------|----------------|---------------------------|----------------|
| | | Rheological | Dielectric (s) |
| TETA ^a | 0 | | |
| | 5.2 | | 6,400 |
| | 10.6 | | 4,980 |
| | 16.2 | | 4,080 |
| | 22.6 | | 4,200 |
| DDM ^a | 0 | | |
| | 5.2 | | 2,640 |
| | 10.6 | | 1,560 |
| | 16.2 | | 1,260 |
| | 22.6 | | 1,020 |

^a For TETA, all measurements were performed at 30°C and for DDM at 80°C.

for pure epoxy resins.³⁹⁻⁴¹ In general, the data obtained have been restricted to observation of frequencies above 10 Hz and usually focused on the variation of the dielectric loss and constant at frequencies of the order of 1 kHz. Variations observed in this region are characteristic of the fluid system undergoing a change to a vitrified state and the main peak observed is that associated with the alpha relaxation—the glass transition process. The dielectric facilities at Strathclyde allow real-time investigation of the frequency range 10^{-1} – 10^5 Hz. This is a much broader frequency range than usually available and reveals the presence of important features that are located at lower frequencies.⁴²

Studies of Cure in DGEBA/TETA Systems

The real-time measurements of the cure in DGEBA/TETA were performed at 30°C (Fig. 3). The initial

high-frequency independent value of the dielectric constant reflects the fact that the monomer dipoles are able to undergo facile rotational motion at frequencies *above* those used in this study. The spikes observed at very low frequency are an artifact of the computer routine used to generate the three-dimensional plots. The large, approximately $1/\omega$ dependence of the dielectric loss reflects the initial high ionic conductivity of the mixture. As cure proceeds, the amplitude of this component decreases markedly, disappearing at the point at which vitrification occurs. The drop in the dielectric constant at about 121 min and also the observation of a *peak* that moves to lower frequency with increasing time reflects the vitrification of the matrix. The peak corresponds to the main dipolar reorientation process, normally designated the alpha process, α , and is associated with the glass transition, T_g . A small dispersion in the dielectric constant and loss located at around 10^4 Hz is associated with the rotational motion of the pendant OH group, generated as a consequence of the curing reaction and is designated the beta process, β .^{26,28,43} This type of behavior is consistent with previous observations on this system.^{15,28,42}

Incorporation of CTBN into the curing system (5.2–22.6 wt %) leads to significant changes being observed in the dielectric spectrum (Fig. 4). The large peak observed initially at low frequency and short times is associated with blocking electrodes.^{23,44} In the fluid resin, charge migration to the electrodes occurs relatively rapidly. If these charges are not discharged at the electrodes, they will create a double layer with an associated dielectric dispersion. As cure proceeds, the rate of charge migration is reduced by the increase in the viscosity of the curing resin and the double layer will thicken to ultimately fill the cell. Changes in the double-layer structure are accompanied by the disappearance of the low-frequency relaxation peak (Fig. 4). As the cure proceeds, an increase in the dielectric constant and loss is observed, indicative of an additional dielectric relaxation contribution being present in the system. This contribution changes slightly with time but is retained in the finally cured materials. Examination of the dielectric loss (Fig. 4) indicates that as cure proceeds, the loss is reduced and this reflects a reduction in the contribution due to ionic conduction that obeys a $1/\omega$ relationship. A decrease in the dielectric constant and also the observation of a peak that moves to lower frequency with cure time reflects the inhibition of the main dipolar relaxation of the system, as is indicative of the vitrification process.²⁸ The additional loss process appearing after about

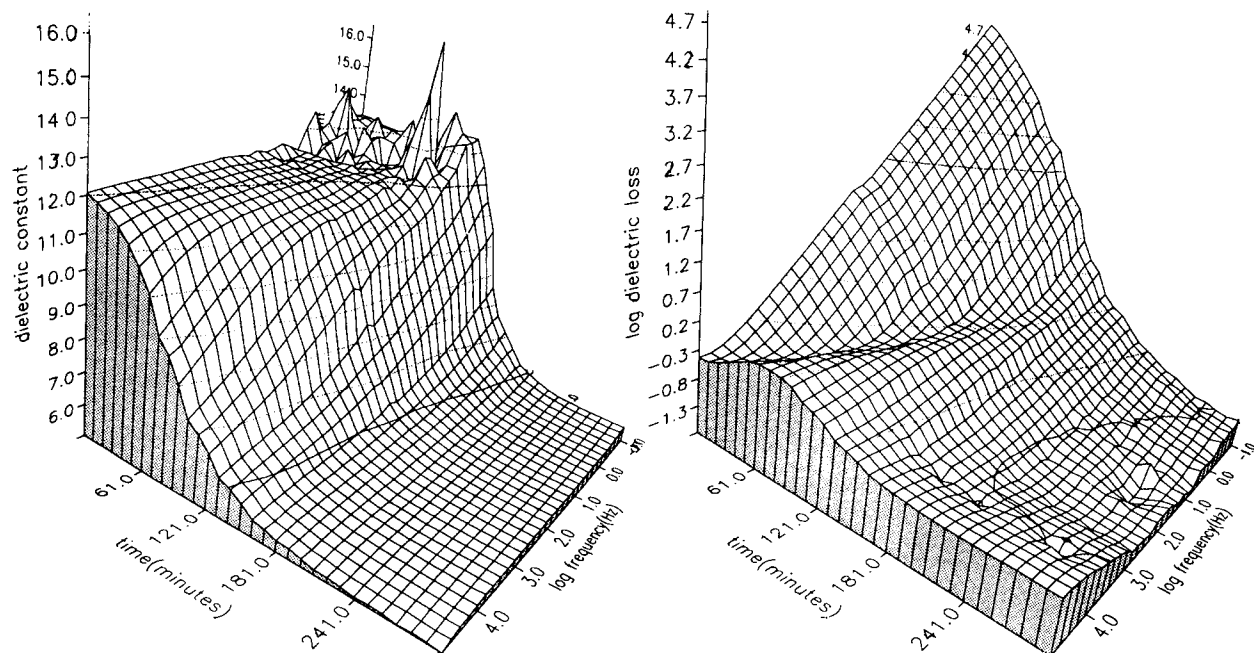


Figure 3 Real-time dielectric constant and loss for the DGEBA/TETA system cured at 30°C.

30 min, observed in the systems containing rubbery occlusions, is indicative of phase separation and is associated with the classical MWS process.^{22–25} The relaxation is associated with charge migration within the rubber domains, the charges being trapped at the less conducting epoxy interfaces. Similar processes have been thoroughly investigated for styrene-butadiene-styrene,⁴⁵ where regular well-defined morphologies are known to exist. The shift of the locus of the relaxation will be discussed later in this paper, but implies that changes are occurring within the occlusions that are influencing the conductivity after the vitrification of the epoxy resin continuum.

Studies of Cure in DGEBA/DDM Systems

A similar investigation to that carried out for the DGEBA/TETA system was carried out for DGEBA/DDM (Fig. 5). Once more, the dielectric traces reflect the initial formation of a blocking electrode system that disappears after about 60 min, a $1/\omega$ dependence of the dielectric loss associated with ionic conduction, and the marked drop in dielectric constant and loss with vitrification after about 80 min. Data were also obtained for a range of concentrations of CTBN; all followed the general trends found in Figure 6 for the 22.6% composition, the main difference being that in this system the

MWS peak does not move with time after the vitrification process.

Comparison of Rheological and Dielectric Behavior

To compare the rheological^{45–47} and dielectric data, it is important to choose a common time-frequency reference, which has to be that used for rheological measurements (2 Hz). Inspection of the dielectric plots (Figs. 3–6) allows estimation of the gelation and vitrification points as discussed previously.^{25,48} In the case of the systems containing CTBN, the increase in the dielectric constant can be used to define the point at which phase separation occurs. Values obtained for the systems studied are presented in Table III, and for the pure resin systems, they agree well with those quoted by other workers.^{25,37–39} Variation of the gelation time and point of phase separation with CTBN content behaves according to an equation of the form

$$t = kV^{-n} \quad (1)$$

where t is the gelation time, k and n are constants characteristic of the system, and V is the volume fraction of the rubbery phase. The coefficients obtained from fitting the data are presented in Table IV. The ratio of t_{gelation} to $t_{\text{phase separation}}$ is approxi-

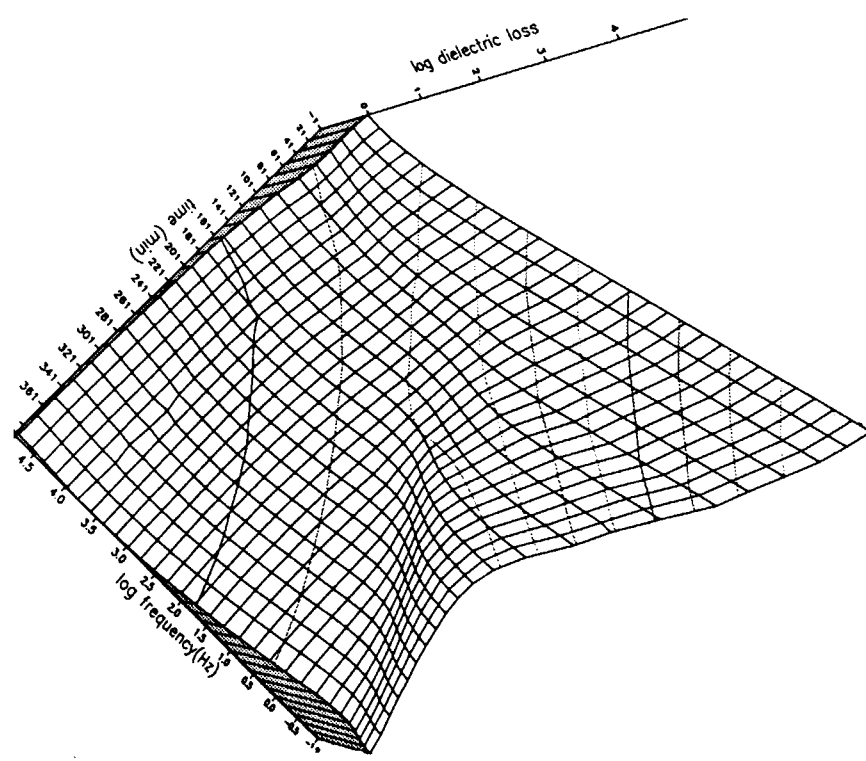
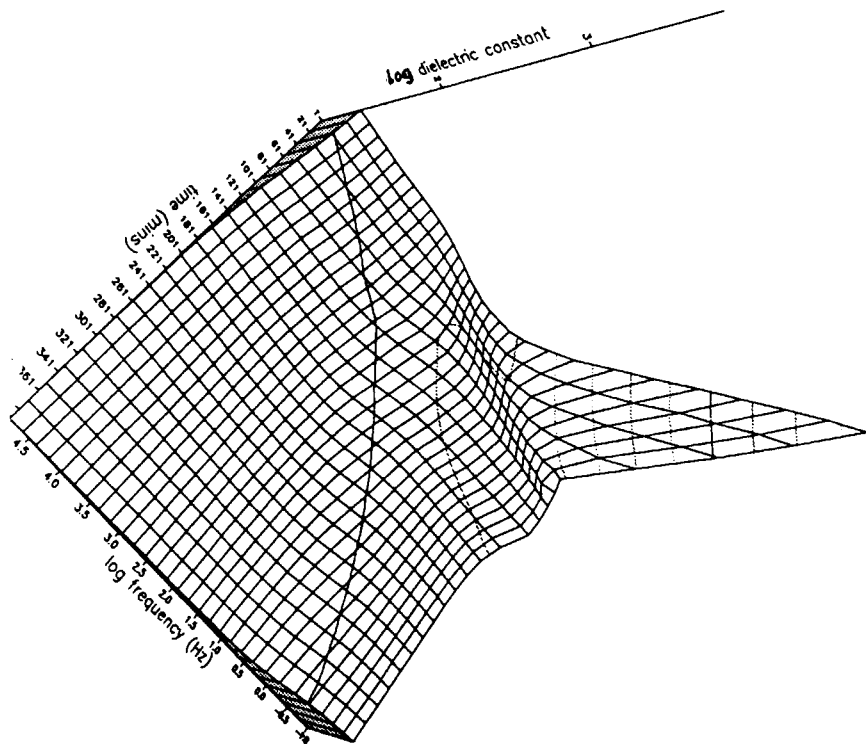


Figure 4 Real-time dielectric constant and loss for the DGEBA/TFEA/22.6 wt % CTBN system cured at 30°C.

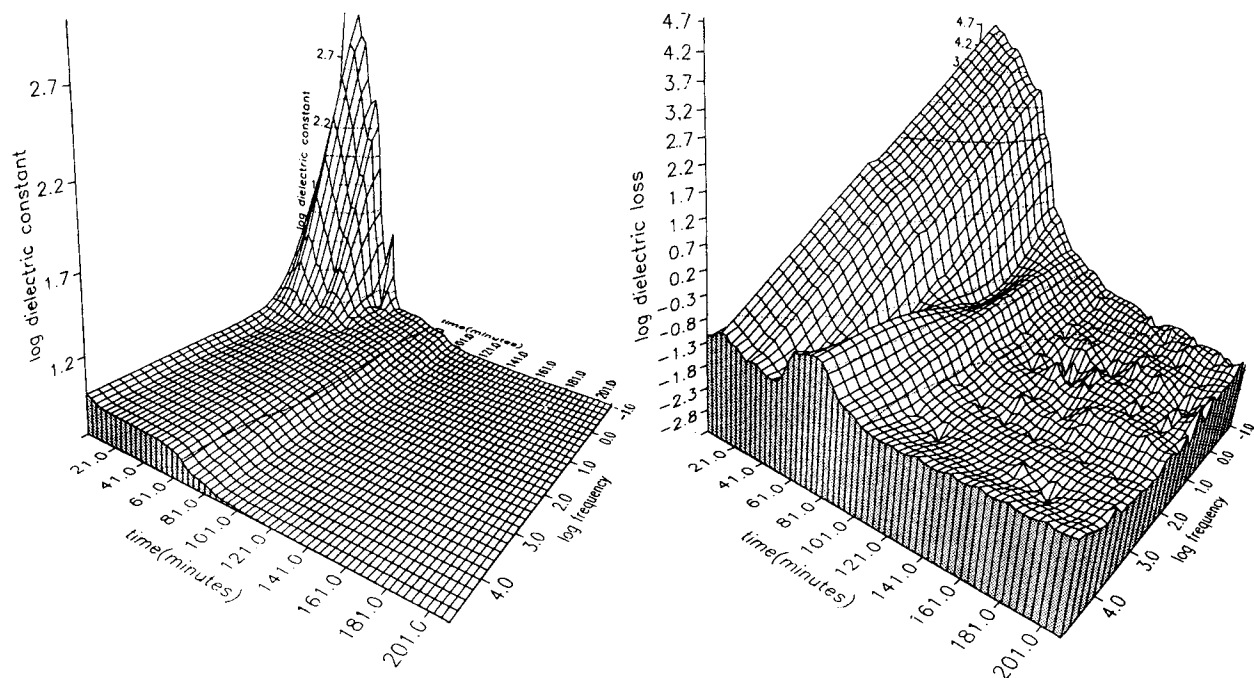


Figure 5 Real-time dielectric constant and loss for the DGEBA/DDM system cured at 80°C.

mately constant with a value of 2.4. The process of phase separation in these systems may be associated with a change in the entropic contribution to the free energy as a consequence of increase in the molecular weight and branched chain structure. Therefore, it is not surprising that one observes an approximately constant ratio for the phase separation and gelation times as they each correspond to a particular value of the viscosity being achieved by the system and will have values that are fixed for a particular type of system.

THEORY FOR THE DIELECTRIC BEHAVIOR OF HETEROGENEOUS SYSTEMS

Phase separation can produce distinct dielectric behavior related to the polarization of mobile charges at the interface between conducting occlusions and the surrounding less conducting matrix. The magnitude of the polarization can be several orders of larger than that observed for dipolar processes. Recent studies of model systems based on doped occlusions of polyethyleneoxide in polycarbonate²² and earlier investigations of styrene-butadiene-styrene,⁴⁵ have shown that the dielectric process is uniquely related to the morphological structure of the material.

The dielectric properties of a polar organic material may be described in terms of the frequency dependence of the complex permittivity^{23,44}:

$$\epsilon^*(\omega) = \epsilon'(\omega) - i\epsilon''(\omega) \quad (2)$$

where $\epsilon'(\omega)$ and $\epsilon''(\omega)$ are the real and imaginary parts of the dielectric permittivity, respectively. In the case of a simple dipolar media, the frequency dependence of eq. (1) has the form

$$\frac{\epsilon'(\omega) - \epsilon'_{\infty}}{\epsilon'_0 - \epsilon'_{\infty}} = \frac{1}{1 + \omega^2\tau^2} \quad (3)$$

and

$$\frac{\epsilon''(\omega)}{\epsilon'_0 - \epsilon'_{\infty}} = \frac{\omega\tau}{1 + \omega^2\tau^2} \quad (4)$$

where ϵ'_0 and ϵ'_{∞} are, respectively, the low- and high-frequency limiting values of the dielectric permittivity for a process with characteristic relaxation time τ . Equations (3) and (4) are interrelated via a Laplace transform according to Kramers Kronig.²³ Analysis of such data to produce information on the dipolar relaxation process has been presented elsewhere.²³

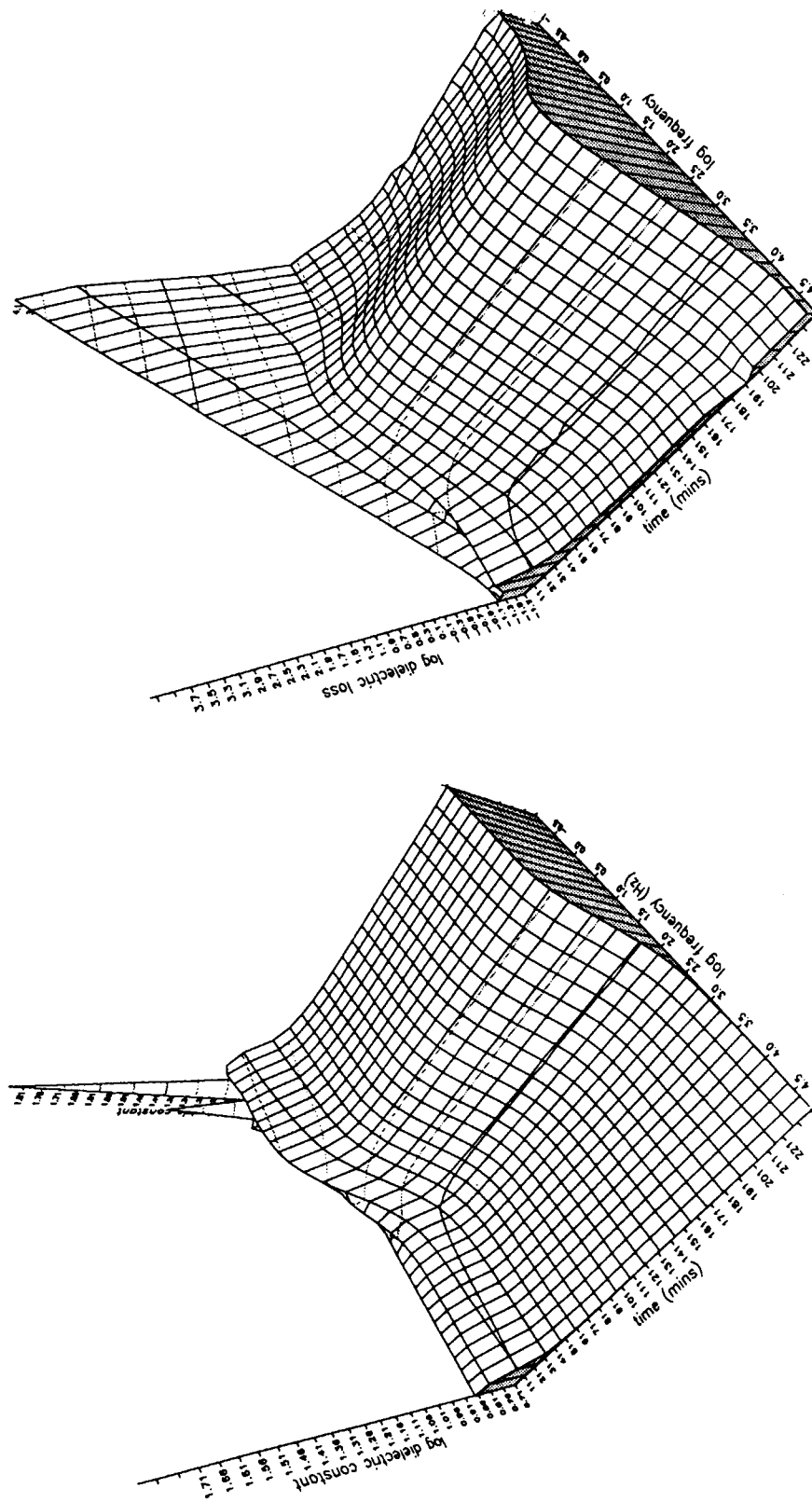


Figure 6 Real-time dielectric constant and loss for the DGEBA/DDM/22.6 wt % CTBN system cured at 80°C.

Table IV The Best-fit Values for k and n Calculated Using Eq. (1)

| Resin DGEBA/ | Process | Coefficients | |
|-----------------|------------------|---------------|-------|
| | | k (seconds) | n |
| DDM | Phase separation | 426 | 0.674 |
| | Gelation | 1396 | 0.431 |

DIELECTRIC PROPERTIES OF HETEROPHASE SYSTEMS

Polarization occurs in heterogeneous dielectrics as a result of the accumulation of charge at the interface between two media having differing permittivities and conductivities. The theory of heterogeneous dielectrics has been reviewed by van Beek.²³ In the case of spheroids of conductivity σ_2 and permittivity ϵ'_2 dispersed in a homogeneous matrix (σ_1, ϵ'_1), the dielectric properties are described by the Maxwell-Wagner-Sillars model (MWS)^{22-25,45}; the characteristic relaxation time τ_{MWS} and low-frequency limiting value of the permittivity ϵ_s are described as follows:

$$\tau_{MWS} = \frac{\epsilon'_1 + \mathbf{A}_a(1 - v_2)(\epsilon'_2 - \epsilon'_1)}{\sigma_1 + \mathbf{A}_a(1 - v_2)(\sigma_2 - \sigma_1)} \quad (5)$$

$$\epsilon_s = \epsilon'_1 \frac{\sigma_1[\mathbf{A}_a(1 - v_2) + v_2](\sigma_2 - \sigma_1)}{\sigma_1 + \mathbf{A}_a(1 - v_2)(\sigma_2 - \sigma_1)} + v_2\sigma_1 \frac{\sigma_1 + \mathbf{A}_a(\sigma_2 - \sigma_1)(\epsilon'_2 - \epsilon'_1) - [\epsilon'_1 + \mathbf{A}_a(\epsilon'_2 - \epsilon'_1)](\sigma_2 - \sigma_1)}{[\sigma_1 + \mathbf{A}_a(1 - v_2)(\sigma_2 - \sigma_1)]^2} \quad (6)$$

and ϵ_∞ is the limiting value of the high-frequency permittivity:

$$\epsilon_\infty = \frac{\epsilon'_1 + [\mathbf{A}_a(1 - v_2) + v_2](\epsilon'_2 - \epsilon'_1)}{\epsilon'_1 + \mathbf{A}_a(1 - v_2)(\epsilon'_2 - \epsilon'_1)} \epsilon'_1 \quad (7)$$

where \mathbf{A}_a is the depolarization factor along the applied field axis, v_2 is the volume fraction of the occluded phase, and the ϵ'_i value is the low-frequency limiting permittivities for phase i . For the special case of spheroids of conductivity σ_2 and permittivity ϵ'_2 dispersed in a homogeneous medium ϵ'_1, σ_1 , the depolarizing factor along the a -axis of the spheroid, A_a has the following form:

For the case of prolate spheroids, $a > b$,

$$\mathbf{A}_a = \frac{-1}{(a/b)^2 - 1} + \frac{a/b}{[(a/b)^2 - 1]^{1.5}} \times \ln\{(a/b) + [(a/b)^2 - 1]^{1/2}\}$$

where a is the length along the major axis, and b , along the minor axis,

For the case of oblate spheroids, $a < b$,

$$\mathbf{A}_a = \frac{1}{1 - (a/b)^2} - \frac{(a/b)}{[1 - (a/b)^2]^{1.5}} \arccos(a/b)$$

and for the case of spheres where $a = b$, $\mathbf{A}_a = 1/3$.

In practical cases, for lossy material dispersed in a polymeric insulator, i.e., $\sigma_2 \gg \sigma_1$ and $v_2 \ll v_1$, the following relationships apply:

$$\tau_{MWS} \simeq \frac{\epsilon'_1 + \mathbf{A}_a(\epsilon'_2 - \epsilon'_1)}{\mathbf{A}_a\sigma_2} \quad (8)$$

$$\epsilon_\infty \simeq \epsilon'_1 \left[1 + v_2 \frac{\epsilon'_2 - \epsilon'_1}{\epsilon'_1 + \mathbf{A}_a(\epsilon'_2 - \epsilon'_1)} \right] \quad (9)$$

Table V Maxwell-Wagner-Sillars Fitting Parameters for Systems Studied

| Sample Code | Conductivity ($\Omega \text{ m}^{-1}$) | Volume Fraction | a/b Ratio | ϵ' |
|-----------------|--|-----------------|-------------|-------------|
| TETA/DEGBA/CTBN | | | | |
| (cure 30°C) | | | | |
| time (min) | | | | |
| 230 | 5E-9 | 0.23 | 1.4 | 5 |
| 370 | 3E-10 | 0.23 | 1.2 | 5 |
| DDM/DEGBA/CTBN | | | | |
| (cure 80°C) | | | | |
| time (min) | | | | |
| 230 | 48 | 0.23 | 1.3 | 7.5 |
| 370 | 1.5E-8 | 0.23 | 1.2 | 7.5 |

Table VI Glass Transitions (T_g) and Activation Energies for DGEBA/TETA/CTBN and DGEBA/DDM/CTBN

| Resin DGEBA/ | CTBN (wt %) | T_g ($^{\circ}\text{C}$) | | Activation Energies (kJ/mol) ³¹ | | Dielectric Increment | |
|-----------------|----------------|------------------------------|------|---|---------------------------------------|----------------------------|----------------------------|
| | | DGEBA | CTBN | DGEBA ^a β Process | CTBN ^a α Process | DGEBA ^b β | CTBN ^b α |
| TETA | 0 | 86 | — | 85 | — | | |
| | 5.2 | 83 | | 79 | 23 | | |
| | 10.6 | 74 | -65 | 72 | 34 | | |
| | 16.2 | 69 | -63 | 72 | 56 | | |
| | 22.6 | 70 | -64 | 71 | 79 | | |
| DDM | 0 | 156 | — | 88 | — | | |
| | 5.2 | 154 | | 84 | — | | |
| | 10.6 | 147 | -66 | 84 | 112 | | |
| | 16.2 | 148 | -62 | — | 108 | | |
| | 22.6 | 147 | -64 | — | 111 | | |

^a The activation energies were obtained from analysis of dielectric data obtained over a frequency range from 10^{-3} to 10^6 Hz and a temperature range from -70 to 170°C . The data have a similar form to that reported by Mangoin and Joshi²⁸ and, therefore, for brevity, the data are not presented in this paper but can be inspected in the MPh thesis of A. S. Vatalis, University of Strathclyde, 1991.³³

^b Dielectric increment derived as the difference between the high- and low-frequency limiting values measured at -30 and -20°C .

Dielectric Measurements

The above theory was used to analyze the data for the DGEBA/TETA/CTBN and DGEBA/DDM/CTBN systems. A good fit of the data was obtained using the input parameters in Table V. The shift of the peak in the case of the TETA/DGEBA/CTBN system during the latter stages of cure can be modeled in terms of changes in the conductivity of the occluded phase. If the occlusions initially are a mixture of partially cured epoxy resin and CTBN forming a single phase, then it is reasonable to assume that the conductivity will be different from that of the pure CTBN phase. As time passes, the epoxy resin will further phase separate to form an included phase. The net result will be a reduction in the overall conductivity of the phase through the introduction of spherical nonconducting epoxy inclusion, as indicated by the fitting parameters (Table VI). The data for TETA indicate that the high viscosity of the rubbery phase is sufficiently large to slow down the migration of the DGEBA and TETA and to reduce the rate of cure within the occlusions. In contrast, DGEBA/DDM/CTBN exhibits a loss peak that changes very little after the vitrification of the main matrix structure (Table V). In this latter system, the mobility of the epoxy resin elements in the rubbery phase will be higher due to the lower viscosity at the higher temperature used in the cure of this system, and as a result, it phase separates and cures at essentially the same time. The fits of

the theory to the data were very good in the case of the DGEBA/DDM/CTBN where the observed peak is only slightly broader than the ideal Debye curve. In the case of the DGEBA/TETA/CTBN, the fit was less satisfactory and this is in agreement with the proposal that in this latter system the precipitation of the DGEBA within the CTBN phase leads to the time-dependent behavior. A better fit of the data could be obtained either by the introduction of a distribution of a/b ratios or by use of a distribution of conductivities. Both modifications of the model could be considered to reflect the heterophase nature of the occluded structures in this system. Further fitting of the data to include these options was not attempted as no obvious basis for selecting one approach over another appears to exist and further studies of this problem are required before a logical choice can be made. The shifts in the conductivity (Table V) are, however, unambiguous and a true reflection of the changes occurring in the system.

Studies of Fully Cured Matrix Materials

Studies were performed over the temperature range -70 to 150°C and over a frequency range from 10^{-3} to 3 MHz. An extensive study of the dipolar relaxations in amine-cured epoxy resins has been reported by Mangion and Johari²⁸ and a similar dielectric relaxation process was observed from measurements

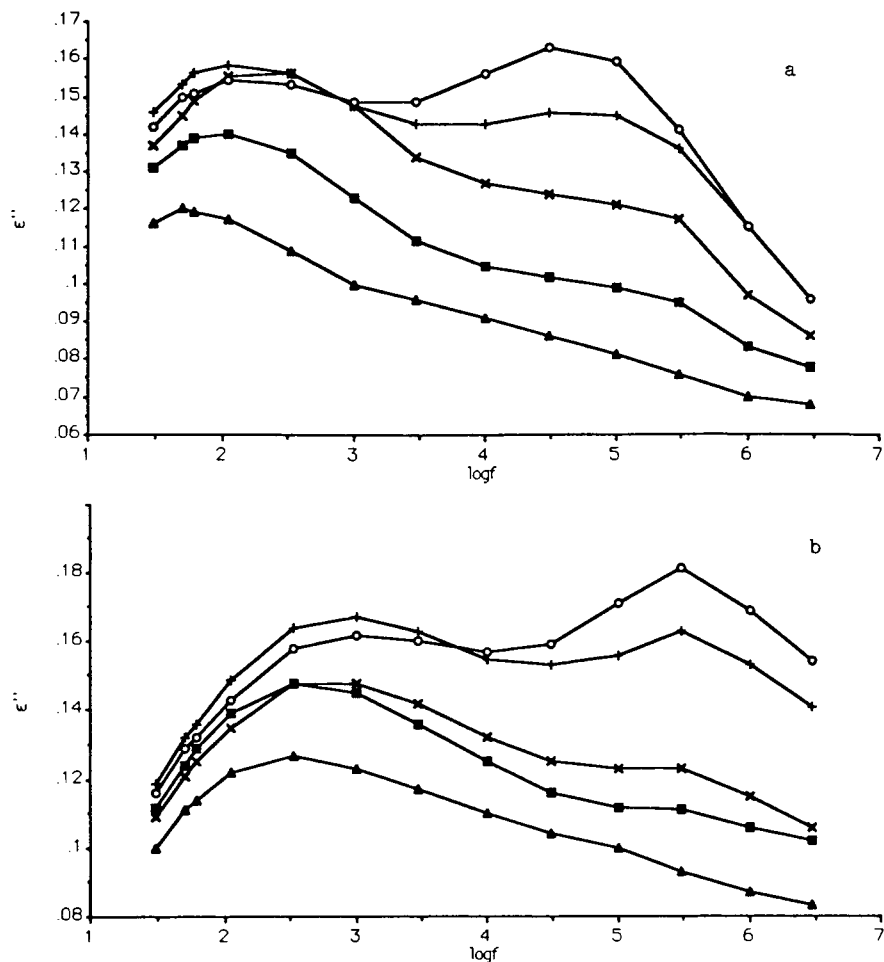


Figure 7 Dielectric loss as a function of frequency for the DGEBA/DDM/CTBN system at (a) -30°C and (b) -20°C . CTBN content (wt %): (Δ) 0, (\square) 5.2, (\times) 10.6, ($+$) 16.2, (\circ) 22.6.

on these systems.³³ The dipolar relaxation is associated with motion of the pendant hydroxyl group generated as a result of ring opening of the epoxy group and undergoes a crankshaft rotational process that also involves the glycidyl portion of the epoxy group.^{47,48} Because of the marked increase in the amplitude of the dipolar process associated with the rotational motion of the acrylonitrile group of the CTBN, above approximately 10 wt %, it was not possible to identify unambiguously the process associated with the epoxy resin matrix and only the α process for the CTBN could be accurately characterized.³³ Using plots of $\tan \delta \{ = \epsilon'' / \epsilon' \}$, it was possible in the case of DGEBA/DDM/CTBN to locate both processes and a set of values for the activation energy of this process were calculated using these data³³ (Table VI). The value obtained for the pure resin is in good agreement with 81.3 kJ/mol quoted by Mangion and Johari²⁸ and Ochi et al.⁴⁷

Changes that occur to the β process can best be compared from plots of the dielectric loss as a function of concentration (Fig. 7 and 8) at -20 and -30°C . In the case of the DGEBA/DDM/CTBN system, addition of CTBN leads to the appearance of a dominant dipolar process associated with the α relaxation, but with a marked reduction in the amplitude of the epoxy relaxation. In the case of the DGEBA/TETA/CTBN system, the growth in the amplitude of the CTBN relaxation occurs without a decrease in the epoxy process. Variation in the magnitude of the epoxy and CTBN relaxation contributions as a function of composition (Figs. 7 and 8), and significant deviations from the expected linear correlation are observed (Table VI). The cure process at low temperatures is sufficiently slow to allow the complete phase separation of the components. In contrast, the increased solubility at higher temperature of the CTBN in the DGEBA/DDM

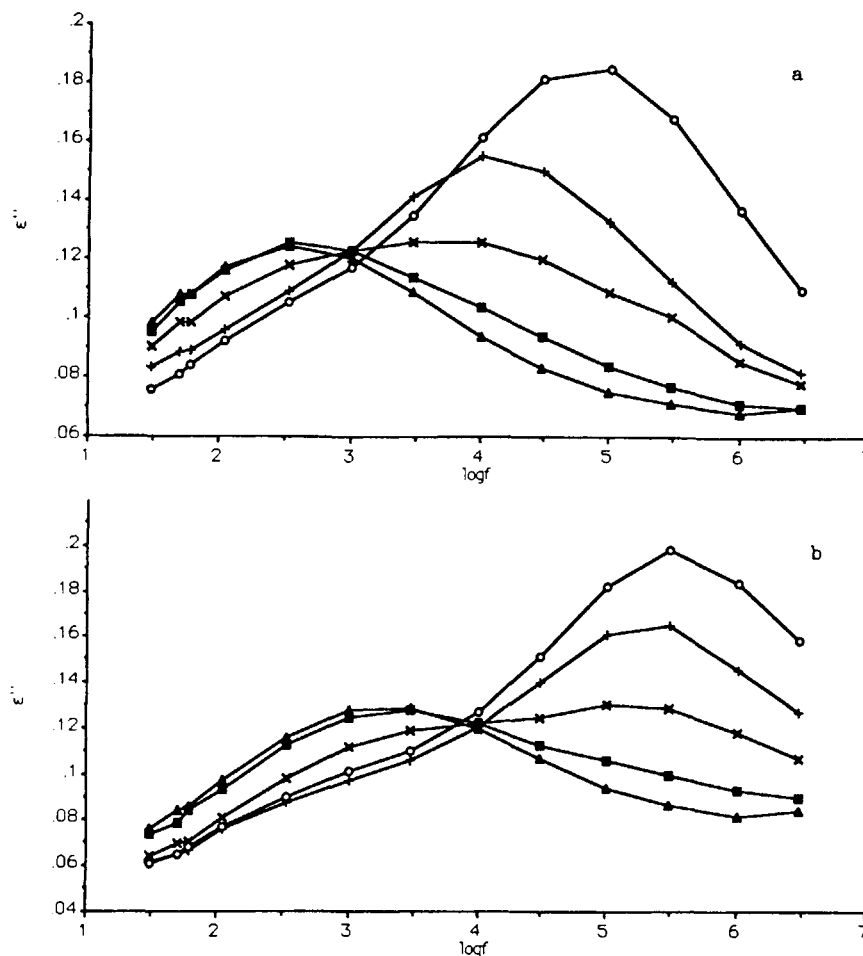


Figure 8 Dielectric loss as a function of frequency for the DGEBA/TETA/CTBN system at (a) -30°C and (b) -20°C . Notation as in Figure 7.

system and the faster rate of cure leads to a situation in which as a result of interaction of the CTBN with the pendant $-\text{OH}$ groups the lower-temperature process becomes combined into the higher-temperature relaxation. Changes in the dielectric spectra indicate that there are differences in nature of the interactions occurring in these systems, reflected in the values of the activation parameters (Table VI), despite the fact that the DSC and SEM measurements would indicate that the components are completely phase-separated.

CONCLUSIONS

This study of CTBN-modified epoxy resins indicates that the dielectric relaxation measurements can give additional information on the nature of the phase structure and interactions occurring in the system

that is not available from other methods. This study also demonstrates the usefulness of the dielectric method for the characterization of dynamic processes occurring in curing systems and also the process of phase separation. Quantitative analysis of the MWS peak can add additional information on the distribution of phase structures present in the system. The dielectric technique opens up the possibility of allowing characterization of the form of the distribution in particle sizes in a phase-separated composite structure and further exploration of the correlation of morphology with mechanical properties.

The authors wish to thank the SERC for assistance with the purchase of the dielectric equipment, Carter Baker Enterprises for the gift of a Mark II version of the Strathclyde Curometer, and the Greek Ministry of Education for financial support for one of us (A. S. V.).

REFERENCES

1. J. Oshima and I. Sasaki, *Polymer News*, Gordon and Breech, New York, 1991, Vol. 16, pp. 198–206.
2. A. M. Donald and E. J. Kramer, *J. Mater. Sci.*, **17**, 1765 (1982).
3. C. B. Bucknall, *Makromol. Chem. Makromol. Symp.*, **16**, 207 (1988).
4. R. J. M. Borggreve, and R. J. Gaymans, *Polymer*, **30**, 71 (1989).
5. S. Wu, *Polymer*, **26**, 1855 (1985).
6. S. Wu, *Polymer Prep. Am. Chem. Soc. Div. Polym. Chem.*, **28**(2) (1987).
7. C. B. Bucknall and A. H. Gilbert, *Polymer*, **30**, 213 (1989).
8. J. N. Sultan and F. J. McGarry, *Polym. Eng. Sci.*, **13**, 29 (1973).
9. A. F. Yee and R. A. Pearson, *J. Mater. Sci.*, **21**, 2462 (1986).
10. A. J. Kinloch, in *Rubber Toughened Plastics*, C. K. Riew, Ed., American Chemical Society, Washington, DC, 1989, p. 222.
11. A. C. Garg and Y. W. Mai, *Compos. Sci. Tech.*, **31**, 179 (1986).
12. R. A. Pearson and A. F. Yee, *J. Mater. Sci.*, **21**, 2475 (1986).
13. L. J. Broutman and G. Panizza, *Int. J. Polym. Mater.*, **1**, 95 (1971).
14. J. H. Daly, R. A. Pethrick, P. Fuller, A. V. Cunliffe, and P. K. Datta, *Polymer*, **22**, 32 (1981).
15. J. H. Daly and R. A. Pethrick, *Polymer*, **22**, 37 (1981).
16. J. H. Daly and R. A. Pethrick, *Polymer*, **23**, 1619 (1982).
17. S. Sankaran and M. Chanda, *J. Appl. Polym. Sci.*, **39**, 1635 (1990).
18. V. Verchere, J. P. Pascault, H. Sautereau, S. M. Moschiar, C. C. Riccardi, and R. J. J. Williams, *J. Appl. Polym. Sci.*, **43**, 293 (1991).
19. S. Sankaran and M. Chanda, *J. Appl. Polym. Sci.*, **39**, 1635 (1990).
20. S. Kunz-Douglass, P. W. R. Beamont, and M. F. Ashby, *J. Mater. Sci.*, **15**, 1109 (1980).
21. E. Butta, G. Levita, A. Marchetti, and A. Lazzeri, *Polym. Eng. Sci.*, **26**, 63 (1986).
22. D. Hawyard, R. A. Pethrick, and T. Siriwittayakorn, *Macromolecules*, to appear.
23. L. K. H. van Beek, *Progr. Dielectrics*, **7**, 69 (1967).
24. R. W. J. Sillars, *Inst. Electr. Eng.*, **80**, 378 (1937).
25. K. W. Wagner, *Arch. Electrotech.*, **2**, 378 (1914).
26. S. D. Senturia and N. F. Sheppard, Jr., *Adv. Polym. Sci.*, **80**, 1 (1986).
27. N. F. Sheppard and S. D. Senturia, *J. Polym. Sci. Part B Polym. Phys.*, **27**, 753 (1989).
28. M. B. Mangion and G. P. Johari, *J. Polym. Sci. Part B Polym. Phys.*, **28**, 71 (1990).
29. D. H. Kaelble, *J. Appl. Polym. Sci.*, **9**, 1213 (1965).
30. D. Kranbuehl, S. Delos, M. Hoff, P. Haverty, W. Freeman, R. Hoffman, and J. Godfrey, *Polym. Eng. Sci.*, **29**, 285 (1989).
31. D. Kranbuehl, P. Haverty, and M. Hoff, *Polym. Eng. Sci.*, **29**, 988 (1989).
32. D. Hayward, M. G. B. Mahoubian-Jones, and R. A. Pethrick, *J. Phys. E. (Sci. Instr.)*, **17**, 683 (1984).
33. A. S. Vatalis, M.Ph., University of Strathclyde, 1991.
34. C. Delides, D. Hayward, R. A. Pethrick, and A. S. Vatalis, *Eur. Poly. J.*, to appear.
35. V. Verchere, J. P. Pascault, H. Sautereau, S. M. Moschiar, C. C. Riccardi, and R. J. J. Williams, *J. Appl. Polym. Sci.*, **42**, 701 (1991).
36. S. M. Moschiar, C. C. Riccardi, R. J. J. Williams, D. Verchere, H. Sautereau, and J. P. Pascault, *J. Appl. Polym. Sci.*, **42**, 717 (1991).
37. A. Vazquez, A. J. Rojas, H. E. Adabbo, J. Borrajo, and R. J. J. Williams, *Polymer*, **28**, 1156 (1987).
38. H. Lee and T. Kyu, *Macromolecules*, **23**, 459 (1990).
39. D. Kranbuehl, S. Delos, E. Yi, J. Mayer, and T. Jarvie, *Polym. Eng. Sci.*, **26**, 338 (1986).
40. J. W. Lane, J. C. Sheferis, and M. A. Bachmann, *Polym. Eng. Sci.*, **26**, 346 (1986).
41. D. R. Day, *Polym. Eng. Sci.*, **26**, 362 (1986).
42. N. F. Sheppard, Jr. and S. D. Senturia, *Polym. Eng. Sci.*, **26**, 354 (1986).
43. L. Didier, J. R. Emery, D. Durrand, D. Hayward, and R. A. Pethrick, *Plastics Rubber and Composites; Processing and Applications*, Elsevier, London, **16**(4), 231 (1991).
44. M. E. Baird, *Electrical Properties of Polymeric Materials*, The Plastics Institute, 1973.
45. A. M. North, R. A. Pethrick, and A. D. Wilson, *Polymer*, **19**, 913 (1978).
46. C. G. Delides, D. Hayward, R. A. Pethrick, and A. S. Vatalis, unpublished data.
47. M. Ochi, M. Shimbo, M. Saga, and N. Takashima, *J. Polym. Sci. Polym. Phys. Ed.*, **24**, 2185 (1986).
48. J. D. Kennan, J. C. Seferis, and J. T. Quinlivan, *J. Appl. Polym. Sci.*, **24**, 2375 (1979).

Received December 18, 1991

Accepted May 13, 1992